Compressed Octahedral Coordination in Chain Compounds Containing Divalent Copper: Structure and Magnetic Properties of $CuFAsF_6$ and $CsCuAlF_6$

Zoran Mazej,*[a] Iztok Arčon,[b] Primož Benkič,[a] Alojz Kodre,[c] and Alain Tressaud[d]

Abstract: Crystal structures and magnetic investigations of $CuFAsF_6$ and $CsCuAlF_6$ are reported. Together with $KCuAlF_6$, these appear to be the only examples of Jahn–Teller pure Cu^{II} compounds containing only one type of ligand that exhibits a compressed octahedral coordination geometry. The Rietveld method has been used for refining the $CsCuAlF_6$ structure based on neutron powder diffraction data at 4 K. The compound crystallizes in space group *Pnma* (no. 62) with $a=7.055(1)$, $b=7.112(1)$, $c=10.153(1)$ Å and $Z=4$ at 4 K. The structure is built from infinite $[CuF_5]_n^{3n-}$ chains of $[CuF_6]^{4-}$ octahedra running along the [100] direction and $(AlF_6)^{3-}$ octahedra connected by corners in the *trans* position, thus giving rise to chains oriented along the [010] direction. Single crystals of $CuFAsF_6$ were prepared under solvothermal conditions in AsF_5 above its critical temperature. The structure was determined from single-crystal data. $CuFAsF_6$ crystallises in the orthorhombic space group *Imma* (No. 74) with $a=10.732(5)$, $b=6.941(3)$, $c=6.814(3)$ Å and $Z=4$ at 200 K. The structure can also be described in terms of one-dimensional infinite $[CuF_5]_n^{3n-}$ chains of tilted $[CuF_6]^{4-}$ octahedra linked by *trans*-vertices running along the *b* axis. The $[CuF_5]_n^{3n-}$ chains are connected through $[AsF_6]^-$ units sharing joint vertices. The compressed octahedral coordination of Cu^{II} atoms in $CuFAsF_6$ and $CsCuAlF_6$ compounds at room temperature is confirmed by Cu K-edge EXAFS (extended x-ray absorption fine structure) analysis. For both compounds strong antiferromagnetic interactions within the $[CuF_5]_n^{3n-}$ chains were observed ($\theta_p=-290\pm10$ K and $\theta_p=-390\pm10$ K for $CuFAsF_6$ and $CsCuAlF_6$, respectively). The peculiar magnetic behaviour of chain compounds containing divalent copper at low temperature could be related to uncompensated magnetic moments in the one-dimensional network.

Keywords: copper · EXAFS spectroscopy · fluorides · Jahn–Teller distortion · magnetic properties · structure elucidation

Introduction

Compounds containing Cu^{II} with its d^9 electron configuration are strongly affected by the Jahn–Teller effect. Hexacoordinate Cu^{II} compounds usually display tetragonal elongation along a fourfold axis with a coordination number (C.N.) 4+2 for Cu^{II}. In the limiting case, a square-planar coordination may be found, as in the $KBrF_4$ type, for example, $CaCuF_4$ and $SrCuF_4$.[1] Although it was initially reported, on the basis of crystallographic data, that some sixfold coordinated Cu^{II} compounds had regular or even tetragonally compressed octahedral coordination, it was later found by other techniques (EPR, EXAFS) that they have the usual Jahn–Teller tetragonally elongated octahedral configuration. More details concerning Jahn–Teller distorted, six-coordinate Cu^{II} complexes may be found in two recently published papers.[2,3]

Beside doped series, such as $Ba_2Zn_{1-x}Cu_xF_6$,[4] one of the rare examples of a compressed geometry is $KCuAlF_6$. Results of the unpolarised low-temperature absorption spectrum of a single crystal,[5] electronic spectra,[6] magnetic measurements[6] and EXAFS[7] are consistent with the crystal structure determined at room temperature[8] and unambiguously confirm the compressed octahedral geometry of

---

[a] Dr. Z. Mazej, Dr. P. Benkič
Department of Inorganic Chemistry and Technology
Jožef Stefan Institute, Jamova 39
1000 Ljubljana (Slovenia)
Fax: (+386) 1-423-2125
E-mail: zoran.mazej@ijs.si

[b] Dr. I. Arčon
Nova Gorica Polytechnic, Vipavska 13
5000 Nova Gorica (Slovenia)

[c] Prof. Dr. A. Kodre
Faculty of Mathematics and Physics
University of Ljubljana, Jadranska 19
1000 Ljubljana (Slovenia)

[d] Dr. A. Tressaud
ICMCB-CNRS, University Bordeaux 1
87, Avenue Dr. A. Schweitzer
33608 Pessac Cedex (France)

DOI: 10.1002/chem.200400397

Cu^{II}. Recently, the energy difference between elongated and compressed geometries of Cu^{II} in tetragonal-layered perovskites was investigated theoretically, by using DFT calculations.[9] $KCuAlF_6$ is one of the rare examples of a pure Cu^{II} compound with only one ligand type and an overall a compressed geometry. In other compounds that have two different ligands, the compression is associated with one ligand having a stronger ligand field than the other.

In this paper we report the crystal structures and magnetic properties of $CuFAsF_6$ and $CsCuAlF_6$, two new examples of Cu^{II} compounds with a compressed tetragonal geometry of Cu^{II}.

Results and discussion

$CuFAsF_6$—X-ray single crystal structure and magnetic properties: $CuFAsF_6$ crystallizes in the orthorhombic space group *Imma* (No. 74) with $a = 10.732(5)$, $b = 6.941(3)$, $c = 6.814(3)$ Å, and $Z = 4$. It should be noted that, although the unit cell constants are similar to those found for $AgFAsF_6$-type compounds,[10,11] the structural arrangement is different. The structure can be described in terms of one-dimensional infinite $[CuF_5]_n^{3n-}$ chains of tilted $[CuF_6]^{4-}$ octahedra (Cu-F-Cu angle = 141.4°) sharing opposite vertices (Figure 1).

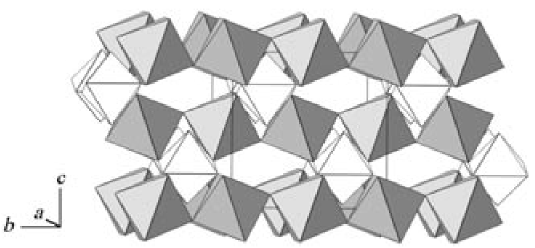

Figure 1. Part of the crystal structure of $CuFAsF_6$ showing one-dimensional infinite $[CuF_5]_n^{3n-}$ chains of tilted $[CuF_6]^{4-}$ octahedra linked by two opposite corners (dark octahedra: $[CuF_6]^{4-}$; light octahedra: $[AsF_6]^-$).

The $[CuF_5]_n^{3n-}$ chains are connected through $(AsF_{4/2}F_2)$ octahedra, in which four bridging fluorine atoms are common to four different $[CuF_6]^{4-}$ octahedra and the remaining two are terminal (Figure 2). The $[CuF_6]^{4-}$ octahedra are compressed, with two shorter Cu–F bonds (2 × 1.838 Å) within the $[CuF_5]_n^{3n-}$ chains and four longer Cu–F(As) bonds (4 × 2.143 Å). Copper is therefore in a rather peculiar environment, with two short bonds and four long ones. The AsF_6 units are close to regular octahedra. As expected, distances between As atoms and bridging F atoms are slightly longer (1.741 Å) than As–F_{ter} (1.686 Å).

Several structural types have been claimed for fluorides with the $A^{II}FM^{V}F_6$ formulation. This series clearly illustrates the variety of coordination numbers found for divalent Jahn–Teller ions such as Cu^{II} and Ag^{II}. Depending on the type of orbital occupied by the single electron of d^9 Ag^{II}, the distortion may lead to a square-planar environment, in which the single electron occupies the $d_{x^2-y^2}$ orbital as in the case of $AgFRuF_6$.[12] In this case, the Ag–F distances are: four at 2.00–2.16 Å and two others at 2.51 Å and 2.66 Å. On the other hand a flattened pentagonal bipyramid has been found for $AgFMF_6$ with M = As, Ir, Au.[10,11,12] For instance, in $AgFAsF_6$ the distances are the following: two Ag–F at 2.00 Å and five Ag–F in the 2.39–2.44 Å range. The resulting near-to-linear coordination is alternatively attributable to the occupancy of the d_{z^2} orbital by the unpaired electron. $CuFAsF_6$ thus illustrates a related possibility: the compressed octahedral coordination.

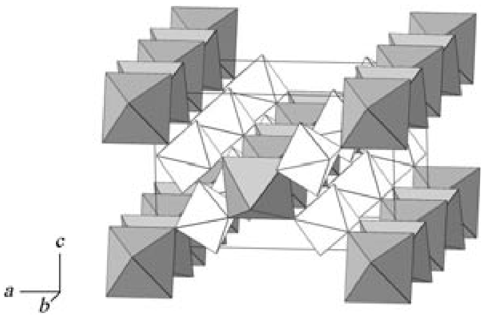

Figure 2. Perspective view of $CuFAsF_6$ showing the packing of one-dimensional infinite chains of $[CuF_6]^{4-}$ octahedra along the *b* axis (dark octahedra: $[CuF_6]^{4-}$; light octahedra: $[AsF_6]^-$).

The thermal dependence of the reciprocal susceptibility of $CuFAsF_6$ is shown in Figure 3 and is similar to that observed for other chain compounds containing divalent copper.[13,14]

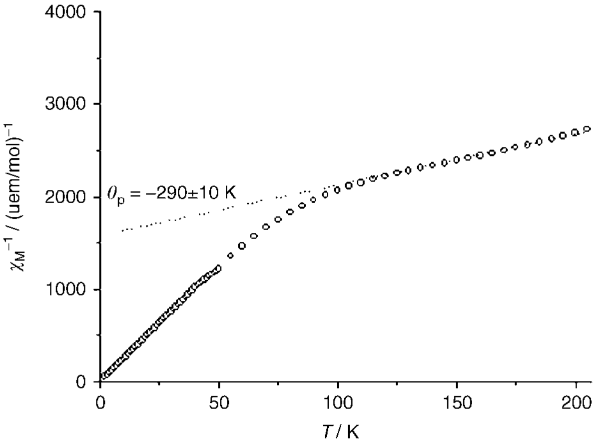

Figure 3. Temperature dependence of the reciprocal magnetic susceptibility of $CuFAsF_6$.

The extrapolated value of the paramagnetic Curie temperature is particularly important: $\theta_p = -290 \pm 10$ K. This value can be related to the significant antiferromagnetic interactions within the $[CuF_5]_n^{3n-}$ chains. The effective moment deduced from the data above 130 K is 1.22 μ_B, which is rather low when compared with the spin-only value of Cu^{II} ($\mu = 1.73$ μ_B). The dependence of the magnetization on the applied field is linear at 4 K, at least up to 25 kOe (Figure 4), accounting for the absence of three-dimensional magnetic ordering at low temperature.

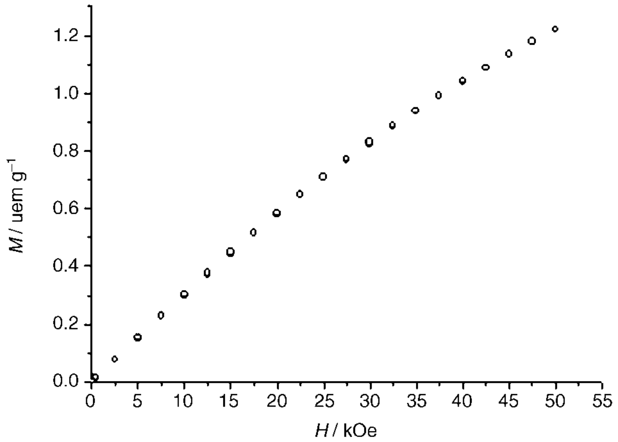

Figure 4. Dependence of the magnetization of $CuFAsF_6$ with the applied field at 4 K.

$CsCuAlF_6$—structure determination from neutron powder diffraction and magnetic properties: The synthesis of $CsCuAlF_6$ was previously reported by Fleisher and Hoppe,[15] but no accurate structure determination was carried out. We have found similar unit-cell constants: a = 7.094(2), b = 7.134(2), c = 10.244(3) Å (*Pnma* space group). In order to determine the structural characteristics of the compound and to verify whether three-dimensional magnetic ordering occurs at low temperature, a neutron diffraction investigation was carried out at 4 K. Diffractograms obtained at 120 K and 4 K are given in Figure 5 together with the difference spectrum. No difference is observed between the two spectra, confirming definitively the absence of any magnetic order at 4 K. Atomic coordinates and thermal factors are given in Table 1, interatomic distances and bonding angles are listed in Table 2. The excellent agreement between the experimental spectrum and the calculated one is demonstrated in Figure 6.

Table 1. Atomic coordinates and thermal factors of $CsCuAlF_6$ at 4 K.

Atom	Site	x	y	z	B_{iso} [Å^2]
Cs	4c	0.482(3)	0.25	0.129(2)	0.30(2)
Cu	4c	0.274(4)	0.25	0.759(2)	0.30(2)
Al	4a	0	0	0	0.30(2)
F1	4c	0.033(4)	0.25	0.678(2)	1.00(2)
F2	4c	0.483(3)	0.25	0.456(2)	1.00(2)
F3	8d	0.150(2)	0.971(2)	0.139(1)	1.00(2)
F4	8d	0.203(2)	0.047(2)	0.895(1)	1.00(2)

Table 2. Interatomic distances [Å] and bonding angles [°] in $CsCuAlF_6$ at 4 K.

Cu–F1	1.88(2)	Al–F2	1.84(2) (2×)
Cu–F1	1.94(2)	Al–F3	1.77(2) (2×)
Cu–F3	2.06(2) (2×)	Al–F4	1.82(2) (2×)
Cu–F4	2.06(2) (2×)	⟨Al–F⟩	1.81(3)
⟨Cu–F⟩	2.01(3)		
F1-Cu-F1	173.6(2)	F2-Al-F2	180.0(2)
F1-Cu-F3	88.8(2) (2×)	F2-Al-F3	87.5(2) (2×)
F1-Cu-F3	87.0(2) (2×)	F2-Al-F3	92.4(2) (2×)
F1-Cu-F4	94.3(2) (2×)	F2-Al-F4	89.0(2) (2×)
F1-Cu-F4	90.3(2) (2×)	F2-Al-F4	90.9(2) (2×)
F3-Cu-F3	99.6(2)	F3-Al-F3	180.0(2)
F3-Cu-F4	85.7(2) (2×)	F3-Al-F4	88.9(2) (2×)
F3-Cu-F4	173.9(2) (2×)	F3-Al-F4	91.1(2) (2×)
F4-Cu-F4	88.9(2)	F4-Al-F4	180.0(2)
Cu-F1-Cu	134.8(2)	Al-F2-Al	150.7(2)

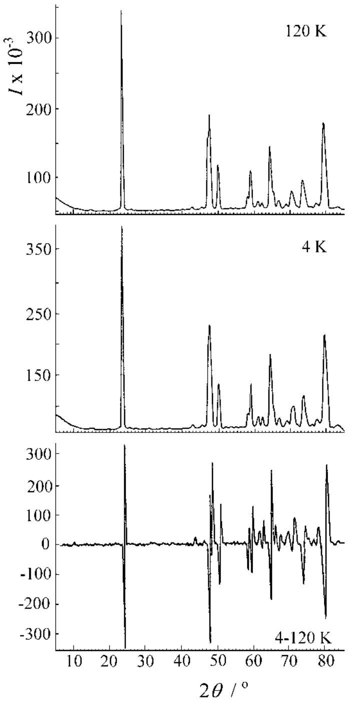

Figure 5. Neutron diffractograms of $CsCuAlF_6$ obtained at 120 and 4 K together with the difference spectrum.

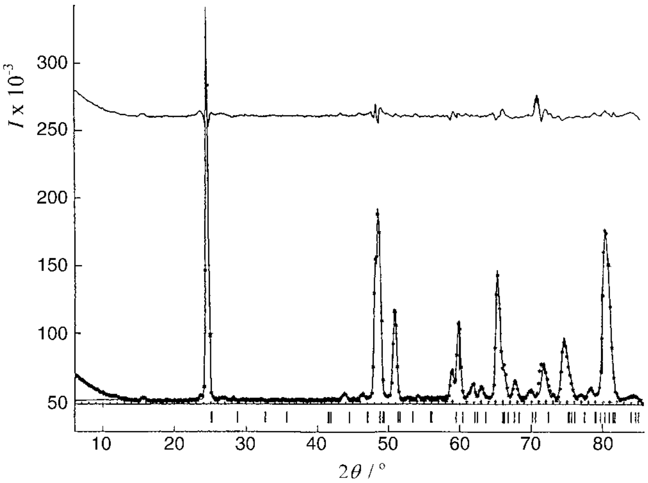

Figure 6. Neutron diffraction profile of $CsCuAlF_6$ at 4 K (***: experimental points; ——: calculated profile; vertical ticks: peak positions of $CsCuAlF_6$; full line above: difference profile).

The structure of $CsCuAlF_6$ is represented in Figure 7. This schematic view shows the two octahedral networks resulting from the ordering between divalent and trivalent cat-

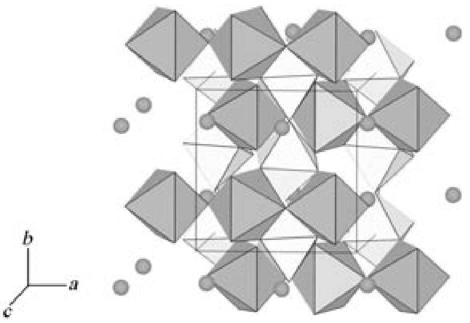

Figure 7. Network of $[CuF_6]^{4-}$ and $[AlF_6]^{3-}$ octahedra in the orthorhombic cell of $CsCuAlF_6$ (dark octahedra: $[CuF_6]^{4-}$; light octahedra: $[AlF_6]^{3-}$; dark spheres: Cs).

ions. The $[CuF_5]_n^{3n-}$ chains run parallel to the [1 0 0] direction, as in the weberite Na_2CuInF_7.[14] $[AlF_6]^{3-}$ octahedra are connected by corners in *trans* positions, giving rise to chains oriented along the [0 1 0] direction. The structure can be considered as being derived from pyrochlore.

The average distance ⟨Cu–F⟩ within $[CuF_6]^{4-}$ octahedra is almost identical to those of Na_2CuInF_7 and Na_2CuGaF_7 weberites, apart from the presence of a C.N. 2+4 configuration. This flattening occurs along the chain direction through the bridging F1 atom (see Table 2).

A significant tilting of these octahedra is observed (Cu-F1-Cu angle = 134.8°), as in the homologous silver compound $CsAgAlF_6$.[16] Similar characteristics are observed for $[AlF_6]^{3-}$ octahedral, which zigzag with an Al-F2-Al angle of 150.7°; however, this feature does not affect the AlF_6 octahedra, which remain undistorted. The average ⟨Al–F⟩ distance of 1.81 Å is the same as that observed in numerous fluoroaluminates. In $CsCuAlF_6$, the F2 atoms are closer to caesium and therefore it is reasonable to assign an 8+2 coordination number to Cs, whereas it is 7+2 and 9 in the isostructural $CsAgAlF_6$ and $CsAgFeF_6$ compounds,[16] respectively, and 10 in $CsNi^{II}Ni^{III}F_6$, as shown below:

- $CsCuAlF_6$: eight distances in the 3.07(1)–3.32(3) Å range; two distances at 3.41(4) Å.
- $CsAgAlF_6$: seven distances in the 3.05–3.17 Å range; two distances at 3.51 Å.
- $CsAgFeF_6$: nine distances in the 3.09–3.31 Å range.
- $CsNiNiF_6$: ten distances in the 3.08–3.28 Å range.

The magnetic behaviour of $CsCuAlF_6$ was measured with a Faraday balance under a constant field of 10 kOe. The thermal dependence of the reciprocal susceptibility shown in Figure 8 is similar to those observed in other chain compounds, such as Na_2CuInF_7 and Na_2CuGaF_7 weberites[14] or Pd^{II}-based compound $CsPdAlF_6$.[17] The extrapolated value of the paramagnetic Curie temperature is: $\theta_p = -390 \pm 10$ K. This value accounts for the significant antiferromagnetic interactions within the $[CuF_5]_n^{3n-}$ chains. The effective moment deduced from the data above 130 K is 1.56 μ_B ($\mu_{calcd} = 1.73$ μ_B, calculated for spin only Cu^{II}).

In addition, we have investigated the magnetic behaviour of an isostructural compound $KCuAlF_6$. The structure of this fluoride was previously solved by Wingefeld and Hoppe. It crystallizes in the same orthorhombic symmetry (*Pnma* space group) with $a = 6.731$, $b = 7.040$ and $c = 9.793$ Å.[8] The structure also consists of tilted chains of compressed CuF_6 octahedra, sharing *trans* corners and connected to AlF_6 octahedra chains running in the perpendicular direction. In the CuF_6 octahedron there are two short Cu–F distances (average distance: 1.877 Å) and four long ones (~2.12 Å). The Cu-F-Cu angle along the chain is equal to 128°. The thermal dependence of the reciprocal susceptibility shows similar features (Figure 9), with a paramagnetic Curie temperature of $\theta_p = -60 \pm 5$ K and an effective moment of about 1.89 μ_B, determined above 100 K. Neutron diffraction experiments have shown that no ordering occurs down to 6 K.

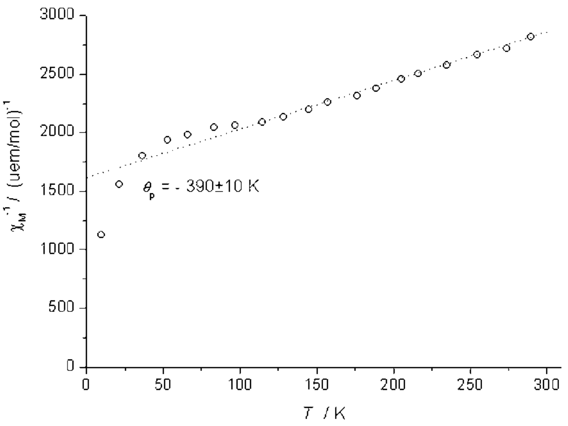

Figure 8. Temperature dependence of the reciprocal magnetic susceptibility of $CsCuAlF_6$.

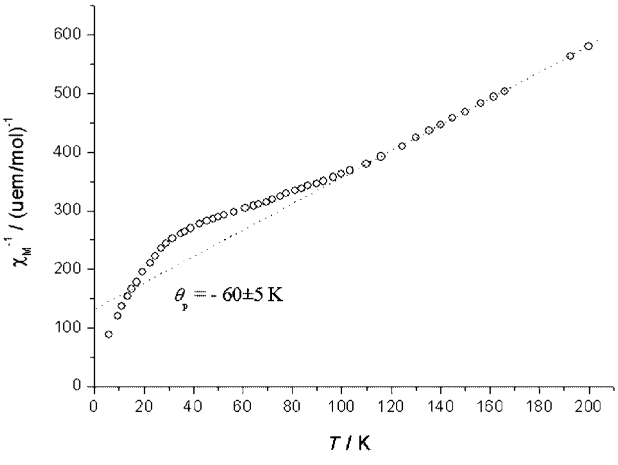

Figure 9. Temperature dependence of the reciprocal magnetic susceptibility of $KCuAlF_6$.

EXAFS analysis of $CuFAsF_6$ and $CsCuAlF_6$: Cu K-edge EXAFS provides information on the local structure around Cu atoms in the sample.[18] We performed EXAFS analysis with the University of Washington UWXAFS package using the FEFF6 code,[19,20] in which the photoelectron scattering paths were calculated ab initio from the presumed distribution of neighbouring atoms around Cu, based on the proposed X-ray/neutron diffraction crystal structure of $CuFAsF_6$ and $CsCuAlF_6$. The EXAFS model of the first Cu coordination shell included all single scattering paths from the central Cu atom to the six (2+4) nearest fluorine atoms in the compressed octahedral geometry, comprising two short and four long Cu–F bonds.

Fourier transformed k^3-weighted Cu EXAFS spectra of the $CuFAsF_6$ and $CsCuAlF_6$ samples are shown in Figures 10 and 11, together with a best-fit EXAFS model of the first coordination shell. Very good agreement between the model and the experimental spectrum is found in the R range from 1.0 to 2.3 Å. Six variable parameters were used in the fit: the amplitude reduction factor S_0^2, the shift of energy origin E_o, two Cu–F distances and two Debye–Waller factors (σ^2), one for the two axial and the other for four equatorial F neighbours. The shell coordination numbers were kept fixed. A complete list of best fit parameters for both compounds is given in Table 3. The quality of fit for the $CuFAsF_6$ spectrum is shown in Figure 10, and for $CsCuAlF_6$ in Figure 11.

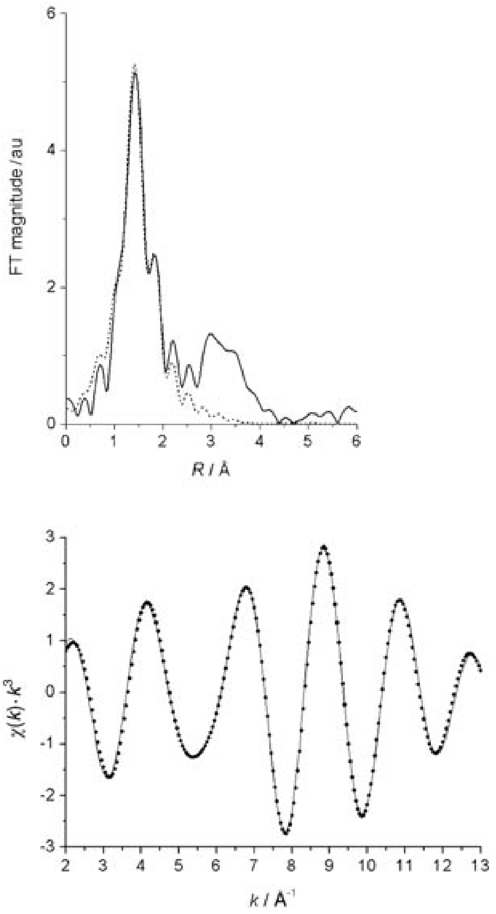

Figure 10. Top: Fourier transform of k^3-weighted Cu EXAFS spectrum of the $CuFAsF_6$ sample, calculated in the k range of 3.0–13.1 Å^{-1}. Experiment: solid line; EXAFS model for the first coordination shell: dashed line. Bottom: Fourier filtered first shell contribution (R range from 1.0 Å to 2.3 Å) of the k^3-weighted Cu EXAFS spectrum of the $CuFAsF_6$ sample. Experiment: dots; best fit EXAFS model for the first coordination shell: solid line.

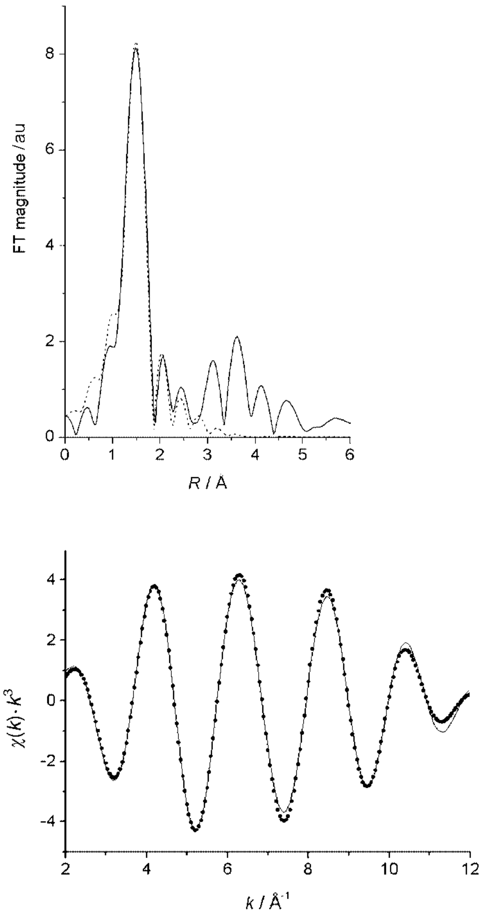

Figure 11. Top: Fourier transform of k^3-weighted Cu EXAFS spectrum of the $CsCuAlF_6$ sample, calculated in the k range of 3.3–11.5 Å^{-1}. Experiment: solid line; EXAFS model for the first coordination shell: dashed line. Bottom: Fourier filtered first shell contribution (R range from 1.0 Å to 2.2 Å) of the k^3-weighted Cu EXAFS spectrum of the $CsCuAlF_6$ sample. Experiment: dots; best fit EXAFS model for the first coordination shell: solid line.

Table 3. Parameters of the nearest coordination shells around copper atoms in $CuFAsF_6$ and $CsCuAlF_6$ compounds obtained by EXAFS analysis. For comparison, Cu–F bond lengths obtained by X-ray or neutron structure determination are also given.

X-ray	EXAFS analysis[a]		
R_{Cu-F} [Å]	R_{Cu-F} [Å]	σ^2 [Å^2]	R factor
$CuFAsF_6$			
1.838(4) (2×)	1.85(1) (2×)	0.003(1)	0.0074
2.143(3) (4×)	2.13(1) (4×)	0.019(2)	0.0074
Neutron	EXAFS analysis[a]		
R_{Cu-F} [Å]	R_{Cu-F} [Å]	σ^2 [Å^2]	R factor
$CsCuAlF_6$			
1.88(2) (1×)	1.91(1) (2×)	0.003(1)	0.0090
1.94(2) (1×)	2.03(3) (4×)	0.029(7)	
2.06(2) (4×)			

[a] Cu–F distance (R_{Cu-F}), and Debye–Waller factor (σ^2). Uncertainty of the last digit is given in parentheses. Best fit is obtained with the amplitude reduction factor $S_0^2 = 0.91 \pm 0.07$ and the shift of energy origin $\Delta E_o = 0.03 \pm 0.5$ eV. The goodness-of-fit parameter, R factor,[20] is given in the last column.

The Cu–F bond lengths obtained for the $CuFAsF_6$ compound (1.85(1) Å for the two axial F and 2.13(1) Å for the four equatorial F neighbours) are in good agreement with the results of the single-crystal X-ray diffraction analysis. The Debye–Waller factors are found to be much lower for the axial (0.003(1) $Å^2$) than for the equatorial F neighbours (0.019(2) $Å^2$). The compressed octahedral coordination of Cu^{II} atoms is also confirmed in the case of the $CsCuAlF_6$ compound, in which the average Cu–F distance for the two axial F neighbours is 1.91(1) Å, and 2.03(3) Å for the four equatorial F neighbours. Again, much lower Debye–Waller factors are found for the axial neighbours (0.003(1) $Å^2$) relative to the equatorial ones (0.029(7) $Å^2$). Similar structural parameters of the first Cu coordination sphere were also found in the case of $KCuAlF_6$.[7]

EXAFS results therefore confirm that the Cu atoms in $CuFAsF_6$ and $CsCuAlF_6$ compounds are located in a compressed octahedral environment at room temperature.

Conclusion

The structures of $CuFAsF_6$ and $CsCuAlF_6$ have been determined by using single-crystal and powder neutron diffraction experiments, respectively. In both cases, the network is composed of one-dimensional infinite $[CuF_5]_n^{3n-}$ chains of $[CuF_6]^{4-}$ octahedra sharing opposite corners. The $[CuF_6]^{4-}$ octahedra exhibit a compressed distortion with two shorter Cu–F bonds within the chain and four longer equatorial Cu–F bonds with connecting (MF_6) octahedra, M = Al, As. A Cu K-edge EXAFS analysis has confirmed that, at room temperature, the Cu^{II} in $CuFAsF_6$ and $CsCuAlF_6$ is in a compressed octahedral environment. It should be emphasized that these fluorides are, together with $KCuAlF_6$, the only examples of pure Cu^{II} compounds containing only one type of ligand in which Cu^{II} is in a tetragonally compressed octahedral coordination. Some examples of Cu^{II}-based fluorides exhibiting various coordination numbers are compared in Table 4. The peculiar magnetic behaviour of these compounds can be related to those of other one-dimensional networks that contain Cu^{II}, in which a non-compensation of magnetic moments may occur at low temperature.

Experimental section

$CuFAsF_6$ was prepared from CuF_2 and excess of AsF_5 in anhydrous hydrogen fluoride as described.[28] The purity of the product was checked by X-ray powder diffraction analysis.

Single crystals of $CuFAsF_6$ were prepared by solvothermal synthesis carried out in a special stainless steel autoclave with a PTFE liner (V = 6 mL). After mixing $CuFAsF_6$ (134 mg), CuF_2 powder (300 mg), AsF_5 (2 g) and aHF (0.4 mmol) in the autoclave, it was heated to 393 K, that is above critical temperature of AsF_5, for 16 days. After cooling to ambient temperature all volatiles were quickly pumped away. The autoclave was opened in a dry-box and single crystals were found in addition to a white colourless solid. Crystals were immersed in perfluorinated oil (ABCR, FO5960) in the dry-box, selected under the microscope and transferred into the cold nitrogen stream of the diffractometer.

Powdered $CsCuAlF_6$ was prepared by the solid-state reaction from a stoichiometric mixture of the three binary fluorides CsF, CuF_2 and AlF_3 at 650 °C in sealed gold tubes for 24 h. The purity of the product was checked by X-ray powder diffraction analysis.

Table 4. Environments of Cu^{II} in various fluorinated networks.

Compound	Axial bond (chain direction) [Å]	Equatorial bond [Å]	Ref.
compressed octahedra (2+4)			
$CuFAsF_6$	1.838 (2×)	2.143 (4×)	[a]
$KCuAlF_6$	1.873/188.1	2.12 (4×)	[8]
$CsCuAlF_6$	1.88/194	2.06 (4×)	[a]
octahedral coordination (2+2+2)			
$KCuCrF_6$	1.872/1.878	2.239/2.26 1.999/2.007	[21]
$CuAuF_5$	1.854 (2×)/2.021 (2×)	2.221 (2×)	[1]
$KCuF_3$	1.888 (2×)/1.962 (2×)	2.258 (2×)	[22,23]
elongated octahedra (4+2)			
CuF_2	1.910 (2×)/1.929 (2×)	2.035 (2×)	[22,24]
Ba_2CuF_6	1.862 (2×)/1.867 (2×)	2.320 (2×)	[22,25]
Cs_2CuF_4	1.933 (2×)/1.961 (2×)	2.474 (2×)	[22,26]
Na_2CuGaF_7	1.936 (2×)/1.945 (2×)	2.100 (2×)	[15]
square planar coordination (4)			
$SrCuF_4$	1.858 (4×)		[1,22,27]

[a] This work.

Single-crystal data of $CuFAsF_6$ were collected on a Mercury CCD area detector coupled with a Rigaku AFC7S diffractometer using monochromatized $Mo_{K\alpha}$ radiation. Data were corrected for Lorentz polarization and absorption effects, and processed using Rigaku Crystalclear software suite program package. The structure was solved by direct methods (SHELXS) and expanded using Fourier techniques. For the results of the structure determination see Table 5. Further details of the crystal structure investigation may be obtained from the Fachinformationszentrum Karlsruhe, 76344 Eggenstein-Leopoldshafen, Germany (fax: (+49)7247-808-666; e-mail: crysdata@fiz-karlsruhe.de), on quoting the depository number CSD-413972.

Neutron diffraction diagrams of $CsCuAlF_6$ were recorded at D1B line of ILL reactor in Grenoble between 4 K and 300 K in the $4 < 2\theta < 84°$ angular range with 2.522 Å wavelength. The results of the structure refinement from the 44 reflections observed in the 4 K diffractogram are given in Table 5.

The magnetic measurements were performed by using a Faraday type balance under a constant field of 10 kOe in the 4–300 K range, and SQUID equipment under various applied magnetic fields.

The Cu K-edge EXAFS data of the $CuFAsF_6$ and $CsCuAlF_6$ were obtained in a standard transmission mode at the E4 station of HASYLAB synchrotron facility, DESY (Hamburg, Germany). The beamline provided a focused beam from an Au-coated mirror and a Si(111) double-crystal monochromator with 1.5 eV resolution at Cu K-edge. Harmonics were effectively eliminated by a plane Au coated mirror and by detuning the monochromator crystal using a stabilization feedback control. Powder samples were sealed between multiple layers of Parafilm® (American Can Company) in a dry-box to prevent hydrolysis. Several layers were stacked to obtain about a unit attenuation above the Cu K-edge and improve the homogeneity. The stack was mounted on a sample holder in a vacuum chamber of the beamline, so that during the measurements the samples were kept in high vacuum at room temperature. The sealed samples were perfectly stable for several hours of the experiment: no sign of hydrolysis was observed after demounting. The stability of the samples was also confirmed by the reproducibility of the consecutive scans in sequence to improve signal-to-noise ratio. The absorption spectra were measured within the −250 to 900 eV region of the Cu K-edge with an integration time of 2 s per step. The exact energy calibration was established with a simultaneous measurement on a Cu metal foil (E_K = 8979 eV) between the second and the third ionization cell.

Table 5. Crystal data and structure refinement for $CuFAsF_6$[a] and neutron diffraction crystal data and structure refinement of $CsCuAlF_6$.

$CuFAsF_6$		$CsCuAlF_6$	
formula	$CuFAsF_6$	formula	$CsCuAlF_6$
M_r [g mol^{-1}]	271.46	T [K]	4
T [K]	200	λ [Å]	2.522
λ [Å]	0.7107	crystal system	orthorhombic
crystal system	orthorhombic	space group	*Pnma* (No. 62)
space group	*Imma* (No. 74)	a [Å]	7.055(1)
a [Å]	10.732(5)	b [Å]	7.112(1)
b [Å]	6.941(3)	c [Å]	10.153(1)
c [Å]	6.814(3)	V [Å^3]	509.4(2)
V [Å^3]	507.6(4)	Z	4
Z	4	2θ range [°]	$4 < 2\theta < 84$
ρ_{calcd} [g cm^{-3}]	3.552	angular step [°]	0.02
μ [mm^{-1}]	10.843	refinement program	DBW 3.2S
$F(000)$	500	collected reflections	44
2θ range [°]	7.0–60.1	refined parameters	25
index ranges	$-11 < h < 15$	profile function	Gauss
	$-7 < k < 9$	FWHM evolution law	$H^2 = U\text{tg}^2\theta + V\,\text{tg}\theta + W$
	$-9 < l < 9$	R_p	0.028
reflections collected	1835	R_{wp}	0.033
independent reflections	392 ($R_{int} = 0.0391$)	R_I	0.023
observed reflections [$I > 2\sigma(I)$]	328		
refinement method	full-matrix least-squares on F^2		
data/restraints/parameters	392/0/28		
goodness-of-fit on F^2	1.115		
final R indices [$I > 2\sigma(I)$]	$R1 = 0.027$/w$R2 = 0.071$		
R indices (all data)	$R1 = 0.033$/w$R2 = 0.073$		
largest diff. peak/hole [e Å^{-3}]	0.720/−1.342		

[a] Crystal structure of $CuFAsF_6$ was first determined on our single crystals with a help of Dr. H. Borrmann, Max-Planck Institut für Chemische Physik fester Stoffe, Dresden (Germany). To obtain better data the determination was repeated on new crystals by one of us (P.B). All crystallographic data presented in this paper are from repeated crystal structure determination.

Acknowledgement

The authors are indebted to J. Darriet for fruitful help in magnetic measurements. Results on $CsCuAlF_6$ have been partly taken from the thesis of N. Ruchaud, co-directed by J. Grannec. The authors gratefully acknowledge the Ministry of Education, Science and Sport of the Republic of Slovenia for the financial support of the present study within the research programs: P1–0045 Inorganic Chemistry and Technology and P1–0112 Study of atoms, molecules and structure by photon and particle impact. The authors also gratefully acknowledge the financial support of the French–Slovenian scientific cooperation programme PROTEUS, the European Commission support IHP-Contract HPRI-CT-1999-00040/2001-00140 and the bilateral project BI-DE/03-04-004 by Internationales Buero des BMBF. Access to synchrotron radiation facilities HASYLAB (project II-01-44) is acknowledged. K. Klementiev of HASYLAB provided expert advice on E4 beamline operation.

---

[1] J. M. Dance, *Mater. Res. Bull.* **1981**, *16*, 599–606.
[2] I. Persson, P. Persson, M. Sandström, A. S. Ullström, *J. Chem. Soc. Dalton Trans.* **2002**, 1256–1265.
[3] M. A. Halcrow, *Dalton Trans.* **2003**, 4375–4384.
[4] C. Freibel, V. Propach, D. Reinen, *Z. Naturforsch. Teil B.* **1976**, *31*, 1574–1584.
[5] K. Finnie, L. Dubicki, E. R. Krausz, M. J. Riley, *Inorg. Chem.* **1990**, *29*, 3908–3910.
[6] M. Atanasov, M. A. Hitchman, R. Hoppe, K. S. Murray, B. Moubaraki, D. Reinen, H. Stratemeier, *Inorg. Chem.* **1993**, *32*, 3397–3401.
[7] V. M. Masters, M. J. Riley, M. A. Hicthman, *J. Synchrotron Radiat.* **1999**, *6*, 242–243.
[8] G. Wingefeld, R. Hoppe, *Z. Anorg. Allg. Chem.* **1984**, *516*, 223–228.
[9] J. M. Garcia-Lastra, J. A. Aramburu, M. T. Barriuso, M. Moreno, *Chem. Phys. Lett.* **2004**, *385*, 286–291.
[10] W. J. Casteel, G. Lucier, R. Hagiwara, H. Borrmann, N. Bartlett, *J. Solid State Chem.* **1992**, *96*, 84–96.
[11] D. Gantar, B. Frlec, D. R. Russel, J. H. Holloway, *Acta Crystallogr. Sect. C* **1987**, *42*, 618–620.
[12] G. Lucier, J. Münzenberg, W. J. Casteel, N. Bartlett, *Inorg. Chem.* **1995**, *34*, 2692–2698.
[13] N. Mercier, M. Leblanc, *Eur. J. Solid State Inorg. Chem.* **1994**, *31*, 423–430.
[14] N. Ruchaud, J. Grannec, P. Gravereau, P. Nuñez, A. Tressaud, *Z. Anorg. Allg. Chem.* **1992**, *610*, 67–74.
[15] T. Fleischer, R. Hoppe, *J. Fluorine Chem.* **1982**, *19*, 529–552.
[16] N. Ruchaud, Ph.D. thesis, University of Bordeaux 1 (France), **1991**.
[17] N. Ruchaud, J. Grannec, A. Tressaud, P. Gravereau, *C. R. Acad. Sci. Ser. IIb* **1995**, *321*, 507–513.
[18] *X-ray Absorption: Principles, Applications, Techniques of EXAFS, SEXAFS and XANES*, *Vol. 92* (Eds.: D. C. Konnigsberger, R. Prins), Chemical Analysis, Wiley, New York **1988**.
[19] J. J. Rehr, R. C. Albers, S. I. Zabinsky, *Phys. Rev. Lett.* **1992**, *69*, 3397–3400.
[20] E. A. Stern, M. Newille, B. Ravel, Y. Yacoby, D. Haskel, *Phys. B* **1995**, *208–209*, 117–120.
[21] D. Kissel, R. Hoppe, *Z. Anorg. Allg. Chem.* **1988**, *557*, 161–170.
[22] B. Müller, *Angew. Chem.* **1987**, *99*, 1120–1135; *Angew. Chem. Int. Ed. Engl.* **1987**, *26*, 1081–1097.
[23] K. Tanaka, M. Komishi, F. Morumo, *Acta Crystallogr. Sect. B* **1979**, *35*, 1303–1308.
[24] J. C. Taylor, P. W. Wilson, *J. Less-Common Met.* **1974**, *34*, 257–259.
[25] H. G. von Schnering, *Z. Anorg. Allg. Chem.* **1973**, *400*, 201–207.
[26] D. Kissel, R. Hoppe, *Z. Anorg. Allg. Chem.* **1986**, *541*, 135–141.
[27] H. G. von Schnering, B. Kolloch, A. Kolodziejezyck, *Angew. Chem.* **1971**, *83*, 440; *Angew. Chem. Int. Ed. Engl.* **1971**, *10*, 413.
[28] B. Frlec, D. Gantar, J. H. Holloway, *J. Fluorine Chem.* **1982**, *20*, 385–396.

Received: April 23, 2004